Hindawi
Journal of Chemistry
Volume 2023, Article ID 7515345, 11 pages
https://doi.org/10.1155/2023/7515345

Research Article

Oil Spill Cleanup Employing Surface Modified Magnetite Nanoparticles Using Two New Polyamines

Mahmood M. S. Abdullah, Mohd Sajid Ali, and Hamad A. Al-Lohedan

Department of Chemistry, College of Science, King Saud University, P.O. Box 2455, Riyadh 11451, Saudi Arabia

Correspondence should be addressed to Mahmood M. S. Abdullah; maltaiar@ksu.edu.sa

Received 10 February 2023; Revised 4 April 2023; Accepted 6 April 2023; Published 18 April 2023

Academic Editor: Mozhgan Afshari

Oil spills in marine environments are a serious environmental concern and using low-cost materials for oil spill cleanup is an emerging subject. In recent years, surface-modified magnetite nanoparticles (MNPs) have shown promising properties for oil spill cleanup due to their high performance, low cost, magnetic properties, and reusability. This study aims to modify the surface of magnetite nanoparticles (MNPs) using two new polyamines and employ them for oil spill remediation. First, tetraethylene glycol (TEG) was converted to the corresponding alkyl halide (AH). Next, two polyamines were synthesized via the alkylation of diamines, 1,11-undecanediamine (UD) and 1,5-pentanediamine (PD), yielding the corresponding AH-UD and AH-PD polyamines. Finally, AH-UD and AH-PD were applied to MNPs' surface modification, yielding the corresponding surface-modified MNPs, AU-MNPs, and AP-MNPs. The performance of AU-MNPs and AP-MNPs for oil spill uptake (OSU%) was investigated using various MNPs-to-oil ratios at different contact times. Furthermore, the reusability of AU-MNPs and AP-MNPs was also investigated over four cycles. The results indicated that the OSU values of AU-MNPs and AP-MNPs were affected by MNPs' ratios and contact time, where their OSU increased as their ratios and contact time increased. In addition, AU-MNPs showed a higher OSU than AP-MNPs, which could be ascribed to the longer alkyl chain in the polyamine (AH-UA) used for their surface modification compared to AP-MNPs. Furthermore, AU-MNPs and AP-MNPs reusability results exhibited effective OSU in four cycles with a relative decline with an increasing number of cycles.

1. Introduction

Various environmental and ecological problems have emerged due to oil spills in recent years [1]. The amount of oil spilled annually is estimated at 4 billion tons globally [2]. A massive oil spill poses a real threat to human health and the environment as a whole. Several remediation techniques have been applied to overcome this disaster, including oil skimmers, oil containment, boom, *in situ* burning, biodegradation, membrane filtration, and chemical dispersants [3–5]. However, these techniques have been limited for oil spill removal due to high implementation costs, low performance, and the generation of secondary pollutants [6]. In recent decades, the use of chemicals, including dispersants and adsorbents, has gained much attention compared with the above-mentioned techniques. In addition to being robust and low-cost, they are highly efficient and have fast remediation [7, 8]. Various chemicals have been used for oil spill remediation, e.g., surfactants, nanoparticles, biosurfactants, and ionic liquids [9–14]. Over the last two decades, several types of nanoparticles have been efficiently applied to oil spill remediation, e.g., titanium dioxide, magnetite, graphite, graphene, carbon nanotubes, and hydrophobic organoclay [14, 15].

Using magnetite nanoparticles (MNPs) for oil spillage remediation has recently received much attention due to their low cost, magnetic character, biocompatibility, and high capacity [7, 16]. However, several problems are associated with using naked MNPs, e.g., oxidation by air and agglomeration. Such issues lead to the loss of MNPs' magnetism and thus reduce their performance for oil spill uptake [17]. Therefore, several chemicals are applied to the

surface modification of MNPs, including organic and inorganic, to avoid these issues [18–20]. Surface modification of MNPs with these materials has shown significant stability, efficient performance for oil spill uptake, and reusability [17]. By modifying the surface of MNPs with hydrophobic materials, they disperse more efficiently in crude oil than in water and thus improve their ability to adsorb crude oil. Our earlier studies used various organic compounds for the modification of MNPs' surface and applied them for oil spill remediation [7, 8, 21, 22]. Herein, two new polyamines were synthesized by converting tetraethylene glycol (TEG) to the corresponding alkyl halide (AH). The obtained alkyl halide was reacted with diamine, 1,11-undecanediamine (UD), and 1,5-pentanediamine (PD) separately in the presence of sodium carbonate, yielding the corresponding polyamines, AH-UD and AH-PD. AH-UD and AH-PD were applied to MNPs' surface modification, yielding the corresponding surface-modified MNPs, AU-MNPs, and AP-MNPs. The performance of AU-MNPs and AP-MNPs for oil spill uptake (OSU%) was investigated using different MNPs-to-oil ratios.

2. Experimental

2.1. Materials. Crude oil was obtained from ARAMCO Co. Its complete specifications were reported in earlier work [23]. 1,5-Pentanediamine (PD, ≥98%) and 1,11-undecanediamine (UD, ≥98%) were obtained from Tokyo Chemical Industry (TCI) Co. Tetraethlyene glycol (TEG, 99%), thionyl chloride (TC), iron (II) chloride tetrahydrate ($FeCl_2.4H_2O$, 98%), iron (III) chloride anhydrous ($FeCl_3 \geq 99.9\%$), sodium carbonate ($Na_2CO_3 \geq 99.5\%$), isopropyl alcohol (≥98%), ethanol absolute, and ammonium hydroxide solution (NH_4OH, 28%) were obtained from Sigma–Aldrich Co.

2.2. Synthesis of Polyamines. For the synthesis of polyamines, AH-UD, and AH-PD, TEG was reacted with the corresponding alkyl halide (AH) using TC, as reported earlier [24]. AH (5.0 g, 21.51 mmol) was added to the stirred solution of diamine, UD (4.0 g, 21.51 mmol), or PD (2.5 g, 21.51 mmol), Na_2CO_3 (1.0 g, 9.43 mmol), and DMF (15 mL) at ambient temperature. The stirring continued for five hours. DMF was evaporated under reduced pressure, followed by dissolving the obtained compound in absolute isopropanol. Polyamines, AH-UD, and AH-PD were obtained after filtration and evaporation of isopropanol under reduced pressure.

2.3. Synthesis of AU-MNPs and AP-MNPs. Solutions of polyamines were prepared by dissolving either AH-UD (4.0 g, 11.61 mmol) or AH-PD (4.0 g, 14.58 mmol) in 200 mL of ethanol. Iron ions solution was prepared by dissolving $FeCl_3$ (9.0 g, 55.49 mmol) and $FeCl_2.4H_2O$ (5.5 g, 27.75 mmol) in 200 mL of distilled water. AH-UD or AH-PD solution was mixed with iron ions solution in a three-neck bottom flask connected to a thermometer and N_2 inlet. After heating the mixture to 50°C, NH_4OH solution (28%, 50 mL) was added dropwise with continuous stirring until the pH reached 10. AU-MNPs and AP-MNPs were obtained after stirring the mixture for a further 1 h, then separated using an external magnet. AU-MNPs and AP-MNPs were dispersed in ethanol and collected by an external magnet several times to remove unreacted polyamines. Finally, AU-MNPs and AP-MNPs were washed with water and dried at ambient temperature.

2.4. Characterization. Fourier-transform infrared (FTIR; Nicolet 6700 spectrometer, Thermo Fisher Scientific Co., USA) spectroscopy was performed to identify the functional groups of the synthesized polyamines and surface-modified MNPs. These compounds were scanned in the spectrum range of 4000-500 cm^{-1}. X-ray diffraction (XRD, BDX-3300 diffractometer, Beijing University Equipment, China) was also used to confirm the structures of AU-MNPs and AP-MNPs. Polyamine structures were also elucidated using nuclear magnetic resonance (^{1}H-NMR, Avance DRX-400 spectrometer, Bruker Co., USA). AU-MNPs and AP-MNPs' thermal stability was investigated by thermogravimetric analysis (TGA, DSC-60, Shimadzu Co., Japan). Heating was performed up to 800°C in a nitrogen atmosphere with a heating rate of 10°C/min.

The morphology and particle sizes (PS) of AU-MNPs and AP-MNPs were investigated using the transmission electron microscopy (TEM, JEM-2100F, Jeol Co., Japan). Furthermore, the PS and polydispersity index (PDI) were measured using the dynamic light scattering technique (DLS, NanoPlus Zeta Potential/Nano Particle analyzer, Malvern Co., UK). Furthermore, contact angle measurements were performed using a drop shape analyzer (DSA, Kruss, Germany) at 25°C to investigate the hydrophobicity of the synthesized MNPs. Finally, the magnetic properties of GO-MNPs and GD-MNPs were confirmed using a vibrating sample magnetometer (VSM, LDJ-9600 Electronics Inc., USA).

2.5. Hydrophobicity of AU-MNPs and AP-MNPs. To investigate the hydrophobicity of AU-MNPs and AP-MNPs, the contact angles of water droplets on their surfaces were measured. This was done by spreading dispersed MNPs (500 mg of either AU-MNPs or AP-MNPs in 2 mL of chloroform) over a glass slide and evaporating the chloroform. After repeating this step several times, a thin film was formed on the glass slide surface. Then, the contact angles of a water droplet on the surface of a glass slide coated with AU-MNPs or AP-MNPs were measured using a drop-shape analyzer (DSA-100).

2.6. Performance of AU-MNPs and AP-MNPs for Oil Spill Uptake. The performance of the as-synthesized MNPs, AU-MNPs, and AP-MNPs (OSU%) was investigated, as reported earlier [7]. Briefly, in a 100 mL beaker, a sample of crude oil (200 mg) was injected on the surface of 70 mL of water. Over the crude oil surface, several amounts of AU-MNPs or AP-MNPs samples (4 mg, 8 mg, 25 mg, 50 mg, 100 mg, and 200 mg) were spread and maintained in contact for different times (3 min, 5 min, 10 min, and 20 min). An external

magnet (a block neodymium magnet $40 \times 25 \times 10$ and the magnetic field produced is 4,300 Gauss) covered with a known-weight plastic film was used for the adsorption of the surface-modified MNPs with adsorbed crude oil on their surfaces. The plastic film with MNPs and crude oil was removed from the external magnet surface, dried, and finally weighed to calculate the weight of the recovered oil. The performance of AU-MNPs and AP-MNPs (OSU%) was calculated using the equation:

$$\text{OSU\%} = \frac{\text{WRO}}{\text{WUS}} \times 100, \quad (1)$$

where WRO and WUS are the weight of recovered oil and used oil, respectively.

The OSU% results were also confirmed using the residual amount of crude oil on the water surface: the residual amount of crude oil on the water surface was extracted using chloroform. Chloroform was evaporated under reduced pressure, and the weight of residual oil was used to calculate OSU%. All measurements were performed in triplicate.

The reusability of the as-synthesized MNPs, AU-MNPs, and AP-MNPs was performed as follows: the used MNPs were collected in a beaker (25 mL), washed three times with chloroform, then with acetone, and finally dried in the air before being used again in the next cycle.

3. Results and Discussion

3.1. Chemical Structures of Polyamines and MNPs. FTIR and ^{1}H-NMR spectroscopies were employed to confirm the formation of polyamines, AH-UD, and AH-PD, as presented in Figures 1(a), 2(a), and 2(b). The spectra of polyamine, AH-UA, and AH-PD (Figure 1(a)) show several characteristic bands belonging to various functional groups. N-H stretching and bending absorption bands are noticed at 3321 cm^{-1} and 1650 cm^{-1}. The stretching absorption bands of C-H methylene appeared at 2926 cm^{-1} and 2856 cm^{-1}, while its bending absorption band appeared at 1462 cm^{-1}. The aliphatic ether (C-O) stretching band is observed at 1110 cm^{-1}. Figures 2(a) and 2(b) show the ^{1}H-NMR spectra of polyamines, AH-UD, and AH-PD. As depicted in the figure, both spectra seem similar except for the integrating alkyl chain methylene groups, where AH-UD has a longer alkyl chain than AH-PD. The protons of the alkyl chain of diamine are noticed at 1.23 ppm and 2.51 ppm, while the etheric (CH_2) protons are observed at 3.5 ppm. The appearance of the alkyl chain of amine and etheric (CH_2) protons confirms the formation of polyamines, HA-UA and HA-PA.

The chemical structures of AU-MNPs and AP-MNPs were elucidated using FTIR and XRD, as shown in Figures 1(b) and 3, respectively. Based on FTIR spectra (Figure 2(b)), polyamines AH-UA and AH-PD appeared at low intensities, indicating surface functionalization of MNPs. Moreover, the appearance of two bands at 578 cm^{-1} and 630 cm^{-1} is attributed to the stretching vibration mode of metal-oxygen (Fe-O) in the crystalline lattice of magnetite, suggesting the formation of MNPs. The formation of surface-modified MNPs, AU-MNPs, and AP-MNPs was also confirmed by XRD diffraction, as presented in Figure 3. The characteristic reflection peaks indicated the formation of pure MNPs with no contamination with other iron oxides. The characteristic peaks appeared at 2 theta: 30.14°, 35.49°, 43.18°, 53.53°, 57.25°, and 62.774° in accordance with Fe_3O_4 database indices (220), (311), (400), (422), (511), (440), and (622). The diffraction patterns matched well with magnetic XRD patterns (JCPDS file No: 00-003-0863). A broad peak at around 2 theta = 20° suggested the presence of polyamines, AH-UA and AH-PD, on the surface of MNPs [21].

3.2. Thermal Stability of AU-MNPs and AP-MNPs. The thermal stability of the synthesized MNPs, AU-MNPs, and AP-MNPs was investigated using TGA, as shown in Figure 4. As depicted in Figure, weight losses at 120°C were 3.18% and 1.96% for AU-MNPs and AP-MNPs, respectively, due to loss of physisorbed water. Afterward, weight losses at 400°C were 11.0% and 7.16% for AU-MNPs and AP-MNPs, respectively. In this region, the weight loss could be attributed to the decomposition of polyamine components on the MNPs' surfaces. The mass loss after 400°C can be linked to the transformation of Fe_2O_3 to FeO by reduction of Fe(III) to Fe(II) with the carbonaceous residual mass [25]. Furthermore, AU-MPNs showed a greater mass loss than AP-MPNs due to the increased amount of AH-UA on the AU-MNPs surface than AH-PD.

3.3. Particle Sizes of AU-MNPs and AP-MNPs. Figures 5 and 6 illustrate the particle sizes of AU-MNPs and AP-MNPs evaluated using TEM and DLS techniques. TEM micrographs (Figures 5(a) and 5(b)) showed irregular MNPs with an average diameter of 10.2 nm for both. Moreover, these micrographs showed the aggregation of MNPs in cluster form due to the magnetic nature of MNPs where these nanoparticles attract each other [26]. Figures 6(a) and 6(b) show particle size and PDI measured using DLS in chloroform. The PS and PDI were 141.8 nm and 0.225, respectively, for AU-MNPs, while 133.4 nm and 0.215 for AP-MNPS, respectively. The difference between the PS measured using this technique and the PS measured by TEM could be explained by the aggregation of MNPs in chloroform due to their magnetic nature.

3.4. Hydrophobicity of AU-MNP and AP-MNPs. MNPs' dispersion is strongly affected by their hydrophobicity. Their dispersion in crude oil increases as their hydrophobicity increases, while it decreases in water as their hydrophobicity increases. Furthermore, MNPs' hydrophobicity promotes their interaction with crude oil components, enhancing their performance in oil spill uptake. Hydrophobicity is measured by contact angle (CA). An increase in the CA value (>90°) of a water droplet on a thin film of MNPs surface indicates an increased hydrophobicity of these nanoparticles. Figures 7(a) and 7(b) show the CA of a water droplet on AU-MNPs and AP-MNPs surfaces, as illustrated in the Experimental section. The CA values were found to be $116° \pm 3$ and $97° \pm 3$ for AU-MNPs and AP-MNPs, respectively. These

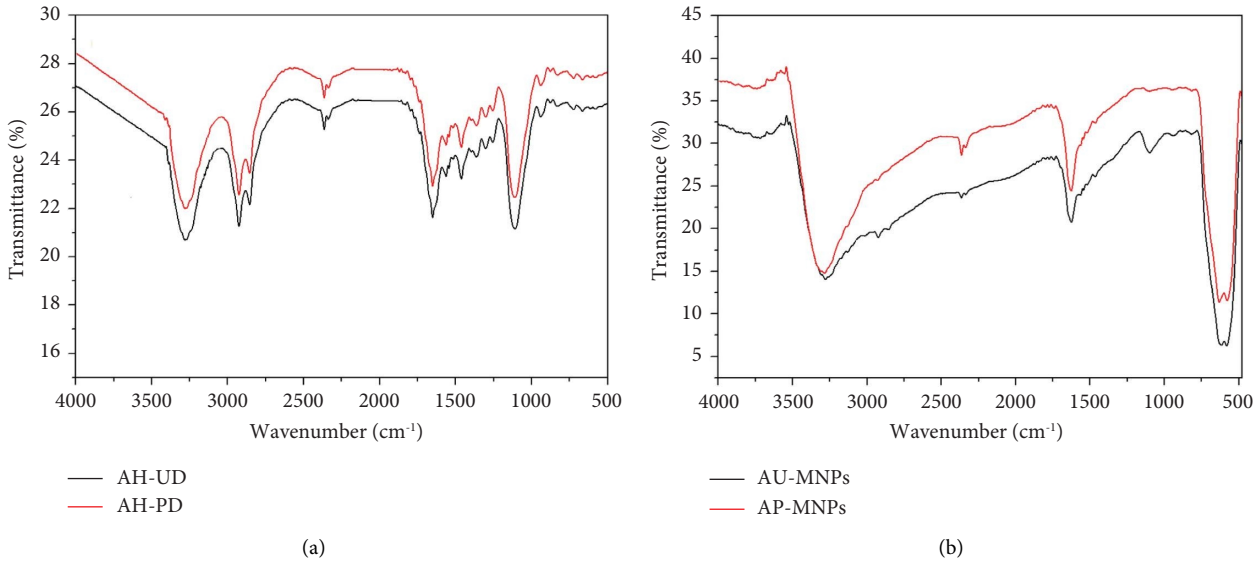

Figure 1: FTIR spectra of (a) polyamine, AH-UD and AH-PD, and (b) MNPs, AU-MNPs, and AP-MNPs.

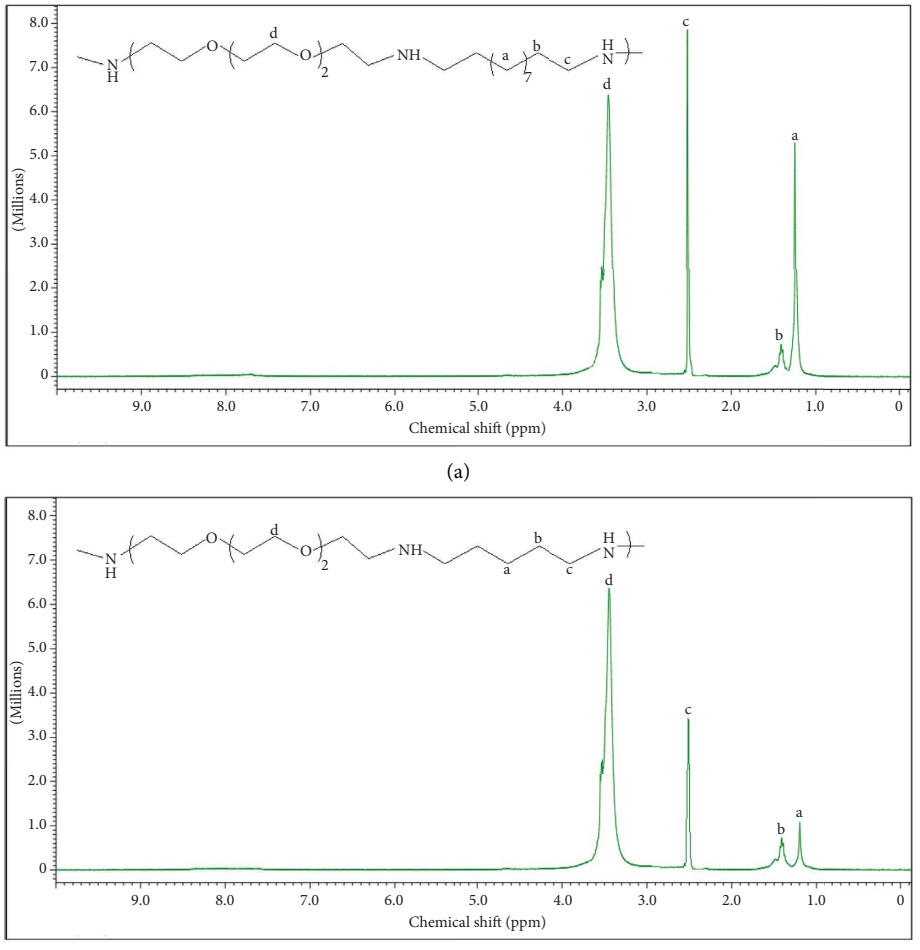

Figure 2: ^{1}H-NMR spectra of (a) AH-UD and (b) AH-PD polyamines.

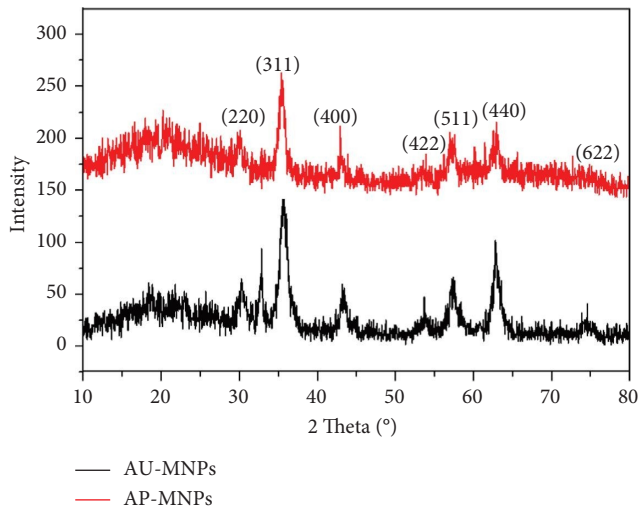

Figure 3: XRD of MNPs, AU-MNPs, and AP-MNPs.

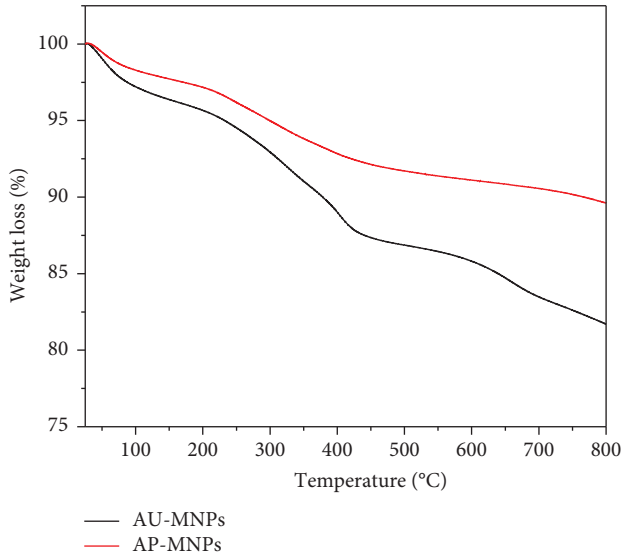

Figure 4: TGA of AU-MNPs and AP-MNPs.

data showed that AU-MNPs and AP-MNPs exhibited high CA, indicating increased hydrophobicity. Furthermore, AU-MNPs displayed a higher CA value than AP-MNPs due to the increased hydrophobicity of the polyamine, AH-UA, used for surface modification of MNPs due to having a longer alkyl chain than AH-PD.

3.5. Magnetization of AU-MNPs and AP-MNPs. For the retrieval of MNPs with crude oil adsorbed on their surfaces, they should respond to an external magnetic field. AU-MNPs and AP-MNPs responded excellently to an external magnet during purification and application. Furthermore, their magnetic properties, including saturation magnetization (Ms), coercivity (Hc), and magnetic remanence (Mr), were measured, as shown in Figure 8. The Ms, Mr, and Hc are 40.23 emu/g, 0.071 emu/g, and 5.5 Oe, respectively, for AU-MNPs, while they are 43.85 emu/g, 0.094 emu/g, and 7.2 Oe, respectively, for AP-MNPs. The Ms values indicate the response of AU-MNPs and AP-MNPs to an external magnet. The low Hc and Mr values suggested the absence of remanence and coercivity at 25°C. Furthermore, AU-MNPs showed a lower magnetization value than AP-MNPs, which could be linked to an increased AH-UA on their surface compared to AP-MNPs, as confirmed by TGA analysis.

3.6. Performance of AU-MNPs and AP-MNPs for Oil Spill Uptake. The dispersity of AU-MNPs and AP-MNPs in low polar solvents with no dispersion in water, high surface area, and response to an external magnet promote their application to oil spill uptake. Therefore, their performance for oil spill uptake was investigated using different MNPs and oil ratios (ranging from 1 : 1 to 1 : 50) at different contact times (ranging from 3 to 20 min), as illustrated in the experimental section. Furthermore, the effect of contact time on OSU was also investigated.

3.6.1. Effect of MNPs : Oil Ratio. The effect of MNPs: oil ratio at 10 minutes is illustrated in Figure 9. The data showed that AU-MNPs and AP-MNPs showed promising OSU even at low ratios. For example, in the MNPs : oil ratio 1 : 1, the OSU of AU-MNPs and AP-MNPs were 100% for both. With the decrease of MNPs ratio to half (MNPs : oil ratio 1 : 2), the OSU of AU-MNPs remained at 100%, while it dropped to 97% with AP-MNPs. After that, as the MNPs ratio decreased, the OSU decreased, reaching 71% and 67% for AU-MNPs and AP-MNPs, respectively, at the MNPs: oil ratio 1 : 50. Furthermore, the data showed that AU-MNPs showed higher OSUs than AP-MNPs, which could be explained by an increase in their hydrophobicity due to the longer alkyl chain in the polyamine (AH-UA) used for their surface modification compared to AP-MNPs.

Figure 10 shows optical images of spilled crude oil on the water's surface. It also shows the dispersed AU-MNPs on the crude oil surface at MNPs : oil ratio 1 : 2 after 10 minutes and collected AU-MNPs using an external magnet with crude oil

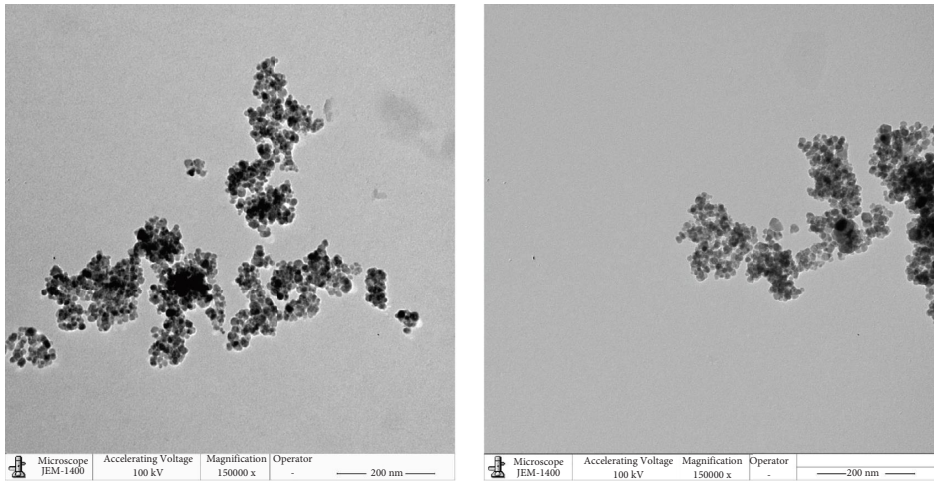

(a) (b)

Figure 5: TEM micrograph of (a) AU-MNP and (b) AP-MNPs.

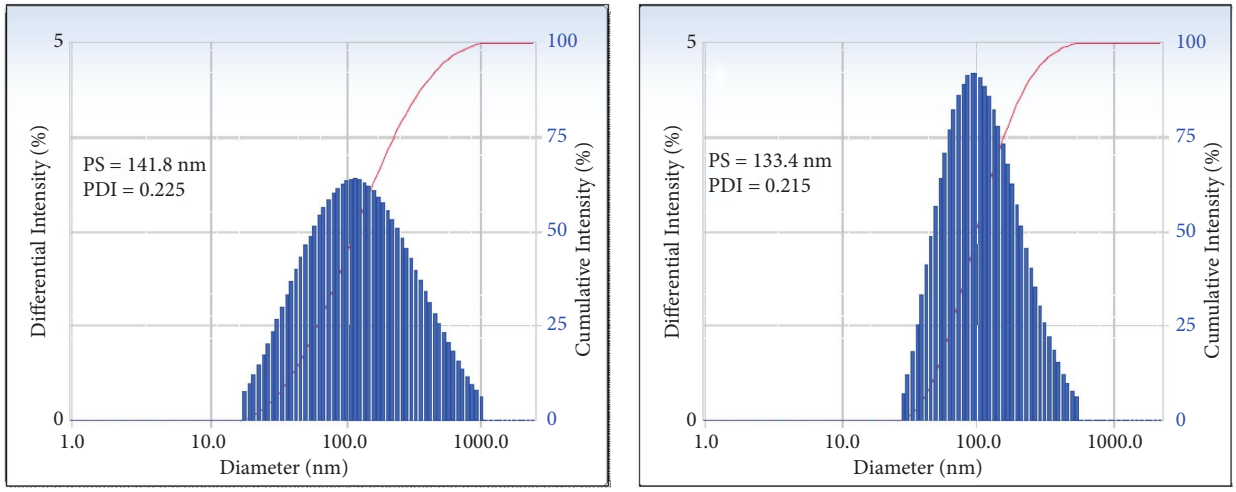

(a) (b)

Figure 6: DLS of (a) AU-MNPs and (b) AP-MNPs.

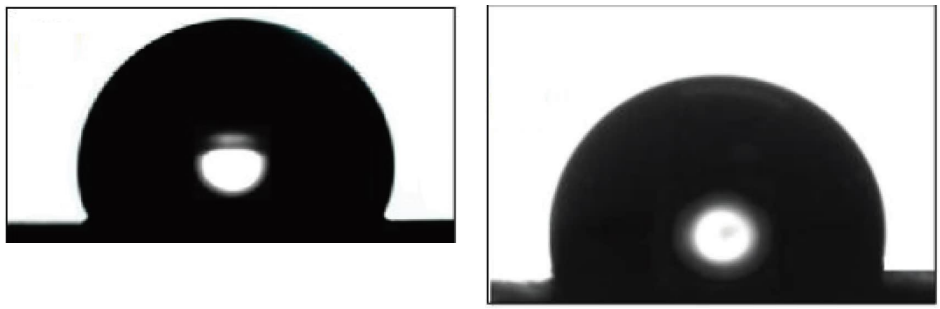

(a) (b)

Figure 7: CAs of a water droplet on (a) AU-MNPs and (b) AP-MNPs surface.

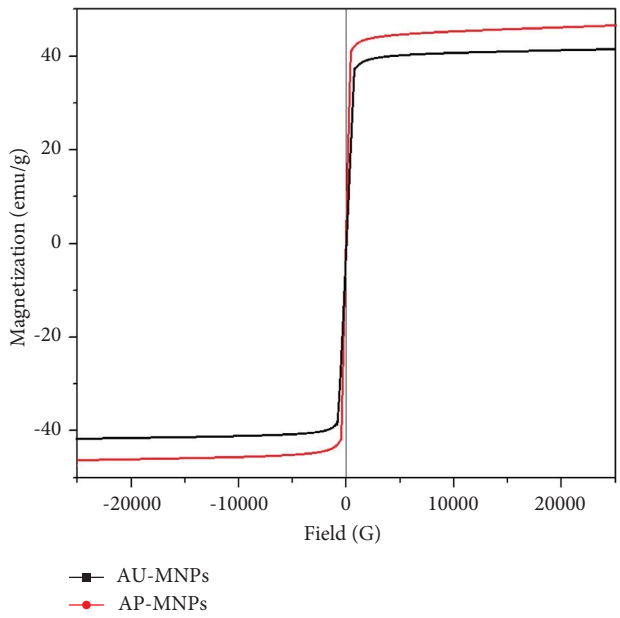

Figure 8: Loop of AU-MNPs and AP-MNPs.

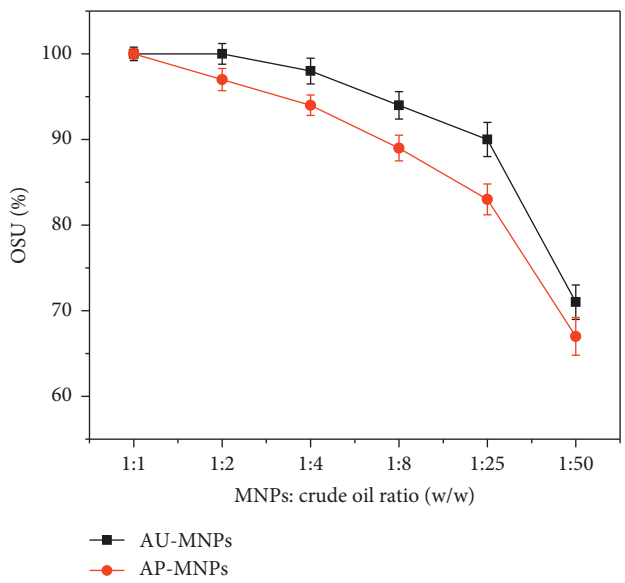

Figure 9: OSU of AU-MNPs and AP-MNPs versus MNPs : oil ratio.

adsorbed on their surface. Figure 10(c) depicts the clarity of water after crude oil removal by applying an external magnet.

3.6.2. Effect of Contact Time. The performance of MNPs for oil spill uptake is greatly affected by contact time [27]. The OSU was investigated at various contact times (3 minutes, 5 minutes, 10 minutes, 15 minutes, and 20 minutes) at a MNPs : oil ratio of 1 : 4, as shown in Figure 11. The data show that as the contact time increased, the OSU of AU-MNPs and AP-MNPs increased to 10 min, reaching 98% and 94%, respectively. An increase in the OSU at the beginning could be ascribed to the many vacant binding sites available on MNPs' surface, which play an essential role in crude oil adsorption. As external MNPs surfaces become saturated, their performance for crude oil uptake slows down until equilibrium is reached [28]. After that, the OSU remained constant with increasing contact time.

Table 1 compares the OSUs of AU-MNPs and AP-MNPs to surface-modified MNPs used for oil spill cleanup in other reported studies. At a high MNPs ratio of 1 : 1, the AU-MNPs and AP-MNPs achieved the highest OSUs compared to other surface-modified MNPs. This reflects the effective dispersity of these MNPs in crude oil, even at high ratios rather than agglomeration. However, they achieved lower OSUs at a low MNPs : crude oil ratio of 1 : 50 in most cases. The interactions between crude oil constituents with AU-MNPs and AP-MNPs include the interactions between oxygen and nitrogen heteroatoms of crude oil constituents and those corresponding on MNPs' surfaces. Additionally, the Van der Waals force is due to the hydrophobic interactions between alkyl chains of diamine and alkyl chains of crude oil components [23].

3.6.3. Reusability of AU-MNPs and AP-MNPs. MNPs have the advantage of being reusable over other materials used for oil spill cleanup. The used MNPs were recollected and washed as reported in the Experimental section. Their reusability at MNPs : oil ratio 1 : 4 and contact time 10 minutes was investigated in four cycles, as shown in Figure 12. As depicted in Figure, the recycled MNPs showed promising OSU compared to the original. However, OSU experienced a relative decline with an increasing number of cycles. For example, the OSUs declined from 98% and 94% in the first cycle to 94% and 89% in the fourth one for AU-MNPs and AP-MNPs, respectively. The decline can be explained by the change in hydrophobicity with increasing cycle numbers [7].

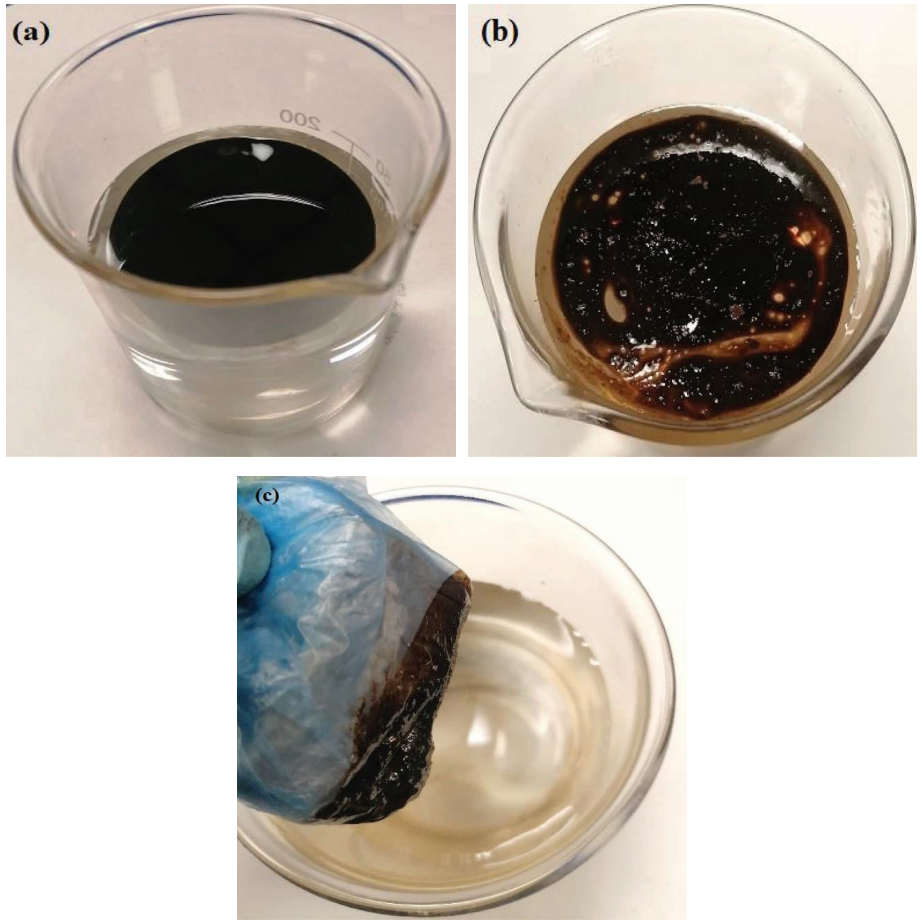

Figure 10: Optical images of (a) oil spill on the water surface, (b) dispersed AU-MNPs on the crude oil surface at a ratio of 1 : 2, and (c) the collected AU-MNPs with crude oil adsorbed on their surface using an external magnet.

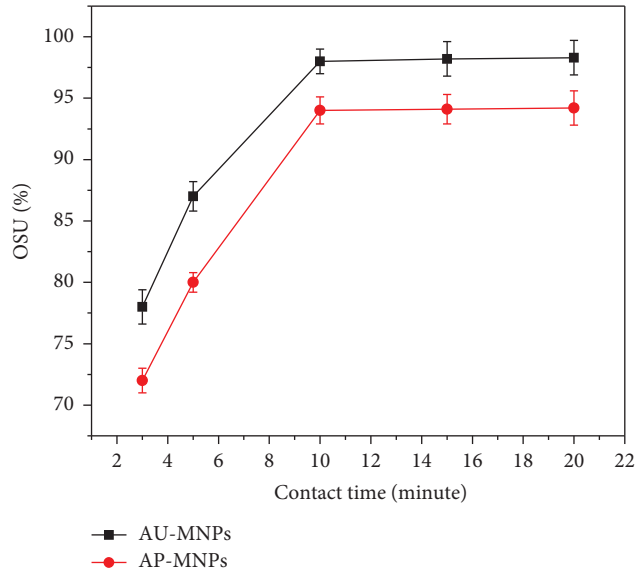

Figure 11: OSU of AU-MNPs and AP-MNPs versus contact time.

Table 1: Compression between OSUs of AU-MNPs and AP-MNPs with surface-modified MNPs used in other studies.

Abbreviation/capping agent	MNPs: crude oil ratio OSU%					
	1 : 1	1 : 8	1 : 10	1 : 25	1 : 50	Reference
Current work AU-MNPs	100	94		90	71	
Current work AP-MNPs	100	89		83	67	
NTEP/Fe_3O_4			90	85	80	[15]
NDETA/Fe_3O_4			87	80	74	[15]
OA-MNPs/amide of alginate	96		93	87	78	[23]
DA-MNPs/amide of alginate	90		87	75	67	[23]
MAE-MNM/*Matricaria aurea* hexane extract	95		92	88	80	[29]
OBE-MNM/*Ochradenus baccatus* hexane extract	91		88	83	76	[29]

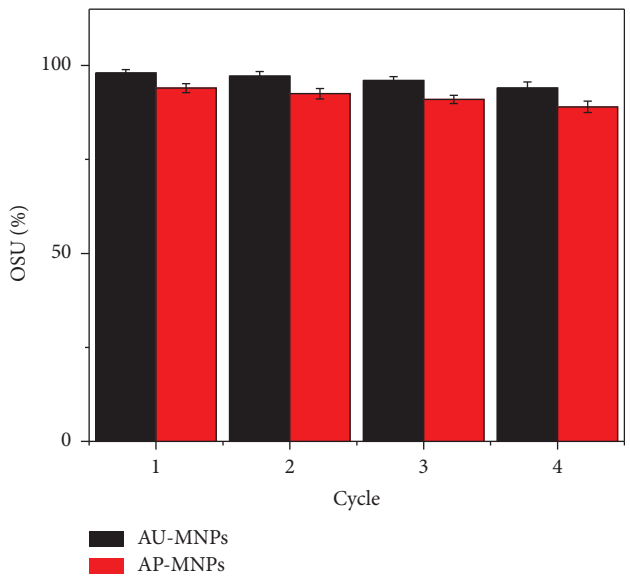

Figure 12: Reusability of AU-MNPs and AP-MNPs in four cycles at MNPs : oil ratio 1 : 4 and contact time 10 minutes.

4. Conclusion

This work synthesized two new low-cost surface-modified MNPs under the short route and mild conditions using two new polyamines. The yielded MNPs were employed for oil spill remediation. First, TEG was converted to the corresponding alkyl halide (AH). Then, the two polyamines were synthesized via the alkylation of diamine, UD, and PD using the obtained AH, producing the corresponding AH-UD and AH-PD polyamines. Finally, AH-UD and AH-PD were applied to the surface modification of MNPs, yielding the corresponding surface-modified MNPs, AU-MNPs, and AP-MNPs. Different techniques were employed to confirm the chemical structures, thermal stability, particle size, hydrophobicity, and magnetic properties of surface-modified MNPs, AU-MNPs, and AP-MNPs. Contact angle and VSM measurements reflected the hydrophobicity of the AU-MNPs and AP-MNPs and their ability to respond to an external magnet.

Thanks to their hydrophobicity and response to the external magnet, AU-MNPs and AP-MNPs were employed for oil spill uptake using a variety of MNPs : oil ratios at different contact times. Increasing the MNP ratio and contact time improved the OSU of AU-MNPs and AP-MNPs. The OSU of AU-MNPs and AP-MNPs improved from 71% and 67%, respectively, at a MNPs : oil ratio of 1 : 50 to 100% for both at a ratio of 1 : 1. Furthermore, the maximum OSU was achieved at a contact time of 10 min, where it reached 98% and 94%, respectively, for AU-MNPs and AP-MNPs at a MNPs : oil ratio of 1 : 4. After this, the OSU remained constant throughout the increasing contact time. This data indicated that the ideal contact time for maximum crude oil adsorption on the MNPs surface is 10 min. Additionally, AU-MNPs achieved higher performance than AP-MNPs due to the longer alkyl chain in the polyamine (AH-UA) used for their surface modification compared to AP-MNPs.

Furthermore, the reusability of AU-MNPs and AP-MNPs was also investigated in four cycles. The recycled AU-MNPs and AP-MNPs showed promising OSU compared to the original; however, there was a relative decline in the OSU with an increasing number of cycles. For example, for AU-MNPs and AP-MNPs, the OSUs decreased from 98% and 94% in the first cycle to 94% and 89% in the fourth cycle. AU-MNPs and AP-MNPs' hydrophobicity changes as the number of cycles increases, causing such a decline. The cumulative analysis of results indicates that synthesizing surface-modified MNPs using low-cost raw materials in a short time and under mild conditions will significantly reduce oil spills in marine environments.

Data Availability

The data are made available upon reasonable request to the corresponding author.

Conflicts of Interest

The authors declare that they have no conflicts of interest.

Authors' Contributions

Mahmood M. S. Abdullah was responsible for the investigation and methodology, conceptualization, writing-original draft, writing-review, and editing the paper. Mohd Sajid Ali was responsible for the investigation and methodology and reviewing and editing the paper. Hamad A. Al-Lohedan was

responsible for the methodology, conceptualization, project administration, and resources.

Acknowledgments

The authors acknowledge the financial support through Researchers Supporting Project number (RSPD2023R688), King Saud University, Riyadh, Saudi Arabia.

References

[1] V.-H. T. Tran and B.-K. Lee, "Novel fabrication of a robust superhydrophobic PU@ ZnO@ Fe3O4@ SA sponge and its application in oil-water separations," *Scientific Reports*, vol. 7, pp. 17520–17612, 2017.

[2] A. Varela, G. Oliveira, F. Souza, C. Rodrigues, and M. Costa, "New petroleum absorbers based on cardanol-furfuraldehyde magnetic nanocomposites," *Polymer Engineering & Science*, vol. 53, no. 1, pp. 44–51, 2013.

[3] H. Neelamegan, D.-K. Yang, G.-J. Lee, S. Anandan, and J. J. Wu, "Synthesis of magnetite nanoparticles anchored cellulose and lignin-based carbon nanotube composites for rapid oil spill cleanup," *Materials Today Communications*, vol. 22, Article ID 100746, 2020.

[4] B. K. Körbahti and K. Artut, "Electrochemical oil/water demulsification and purification of bilge water using Pt/Ir electrodes," *Desalination*, vol. 258, no. 1-3, pp. 219–228, 2010.

[5] D. P. Prendergast and P. M. Gschwend, "Assessing the performance and cost of oil spill remediation technologies," *Journal of Cleaner Production*, vol. 78, pp. 233–242, 2014.

[6] S. B. Hammouda, Z. Chen, C. An, K. Lee, and A. Zaker, "Buoyant oleophilic magnetic activated carbon nanoparticles for oil spill cleanup," *Cleaner Chemical Engineering*, vol. 2, Article ID 100028, 2022.

[7] M. M. Abdullah, N. A. Faqihi, H. A. Al-Lohedan, Z. M. Almarhoon, and F. Mohammad, "Fabrication of magnetite nanomaterials employing novel ionic liquids for efficient oil spill cleanup," *Journal of Environmental Management*, vol. 316, Article ID 115194, 2022.

[8] M. M. Abdullah and H. A. Al-Lohedan, "Fabrication of environmental-friendly magnetite nanoparticle surface coatings for the efficient collection of oil spill," *Nanomaterials*, vol. 11, p. 3081, 2021.

[9] D. Cardona, K. Debs, S. Lemos et al., "A comparison study of cleanup techniques for oil spill treatment using magnetic nanomaterials," *Journal of Environmental Management*, vol. 242, pp. 362–371, 2019.

[10] W. L. da Silva and J. H. Z. dos Santos, "Applications of ionic liquids in environmental remediation," *Green Sustainable Process for Chemical and Environmental Engineering and Science*, Elsevier, Amsterdam, Netherlands, 2021.

[11] B. Doshi, M. Sillanpää, and S. Kalliola, "A review of bio-based materials for oil spill treatment," *Water Research*, vol. 135, pp. 262–277, 2018.

[12] M. U. H. Shah, M. Moniruzzaman, A. V. B. Reddy, M. M. R. Talukder, S. B. Yusup, and M. Goto, "An environmentally benign ionic liquid based formulation for enhanced oil spill remediation: optimization of environmental factors," *Journal of Molecular Liquids*, vol. 314, Article ID 113603, 2020.

[13] M. U. H. Shah, A. V. B. Reddy, and M. Moniruzzaman, "Ionic liquid–based surfactants for oil spill remediation," *Ionic Liquid-Based Technologies for Environmental Sustainability*, Elsevier, Amsterdam, Netherlands, 2022.

[14] B. Singh, S. Kumar, B. Kishore, and T. N. Narayanan, "Magnetic scaffolds in oil spill applications," *Environmental Sciences: Water Research & Technology*, vol. 6, no. 3, pp. 436–463, 2020.

[15] A. O. Ezzat, M. S. Ali, and H. A. Al-Lohedan, "Synthesis, characterization, and application of magnetite nanoparticles coated with hydrophobic polyethyleneimine for oil spill cleaning," *Journal of Chemistry*, vol. 2022, Article ID 3368298, 10 pages, 2022.

[16] H. Zhang, X. Zhong, J.-J. Xu, and H.-Y. Chen, "Fe_3O_4/polypyrrole/Au nanocomposites with core/shell/shell structure: synthesis, characterization, and their electrochemical properties," *Langmuir*, vol. 24, no. 23, pp. 13748–13752, 2008.

[17] A. H. Lu, E. L. Salabas, and F. Schüth, "Magnetic nanoparticles: synthesis, protection, functionalization, and application," *Angewandte Chemie International Edition*, vol. 46, no. 8, pp. 1222–1244, 2007.

[18] K. Qiao, W. Tian, J. Bai et al., "Application of magnetic adsorbents based on iron oxide nanoparticles for oil spill remediation: a review," *Journal of the Taiwan Institute of Chemical Engineers*, vol. 97, pp. 227–236, 2019.

[19] W. Wu, Q. He, and C. Jiang, "Magnetic iron oxide nanoparticles: synthesis and surface functionalization strategies," *Nanoscale Research Letters*, vol. 3, no. 11, pp. 397–415, 2008.

[20] D. F. Enache, E. Vasile, C. M. Simonescu et al., "Cysteine-functionalized silica-coated magnetite nanoparticles as potential nanoadsorbents," *Journal of Solid State Chemistry*, vol. 253, pp. 318–328, 2017.

[21] D. C. Culita, L. Patron, O. Oprea et al., "Detailed characterization of functionalized magnetite and ascertained effects," *Journal of Nanoparticle Research*, vol. 15, no. 9, pp. 1–15, 2013.

[22] M. M. Abdullah, H. A. Al-Lohedan, and A. M. Atta, "Novel magnetic iron oxide nanoparticles coated with sulfonated asphaltene as crude oil spill collectors," *RSC Advances*, vol. 6, no. 64, pp. 59242–59249, 2016.

[23] M. M. Abdullah, A. M. Atta, H. A. Allohedan, H. Z. Alkhathlan, M. Khan, and A. O. Ezzat, "Green synthesis of hydrophobic magnetite nanoparticles coated with plant extract and their application as petroleum oil spill collectors," *Nanomaterials*, vol. 8, p. 855, 2018.

[24] M. M. Abdullah and H. A. Al-Lohedan, "Alginate-based poly ionic liquids for the efficient demulsification of water in heavy crude oil emulsions," *Fuel*, vol. 320, Article ID 123949, 2022.

[25] M. M. Abdullah and H. A. Al-Lohedan, "Novel amphiphilic gemini ionic liquids based on consumed polyethylene terephthalate as demulsifiers for Arabian heavy crude oil," *Fuel*, vol. 266, Article ID 117057, 2020.

[26] M. Masuku, L. Ouma, and A. Pholosi, "Microwave assisted synthesis of oleic acid modified magnetite nanoparticles for benzene adsorption," *Environmental Nanotechnology, Monitoring & Management*, vol. 15, Article ID 100429, 2021.

[27] C. Schweiger, C. Pietzonka, J. Heverhagen, and T. Kissel, "Novel magnetic iron oxide nanoparticles coated with poly (ethylene imine)-g-poly (ethylene glycol) for potential biomedical application: synthesis, stability, cytotoxicity and MR

imaging," *International Journal of Pharmaceutics*, vol. 408, no. 1-2, pp. 130–137, 2011.

[28] K. B. Debs, D. S. Cardona, H. D. da Silva et al., "Oil spill cleanup employing magnetite nanoparticles and yeast-based magnetic bionanocomposite," *Journal of Environmental Management*, vol. 230, pp. 405–412, 2019.

[29] E. M. Soliman, S. A. Ahmed, and A. A. Fadl, "Adsorptive removal of oil spill from sea water surface using magnetic wood sawdust as a novel nano-composite synthesized via microwave approach," *Journal of Environmental Health Science and Engineering*, vol. 18, no. 1, pp. 79–90, 2020.

[30] M. M. Abdullah, A. M. Atta, H. A. Al-Lohedan, H. Z. Alkhathlan, M. Khan, and A. O. Ezzat, "Synthesis of green recyclable magnetic iron oxide nanomaterials coated by hydrophobic plant extracts for efficient collection of oil spills," *Nanomaterials*, vol. 9, no. 10, Article ID 1505, 2019.